Applied Physics A (2020) 126:514
https://doi.org/10.1007/s00339-020-03630-2

Applied Physics A
Materials Science & Processing

Theoretical study of the structures and electronic properties for NiX (X = Na–Cl) clusters

Wei Song[1,2] · Peng-fei Ma[2] · Zhe Fu[3] · Jin-long Wang[3] · Wei Zhang[4]

Received: 31 August 2019 / Accepted: 13 May 2020 / Published online: 11 June 2020

Abstract

Using the first-principles calculations, we study the structural, electronic and magnetic properties of the neutral and ionic $Ni_{n-1}X$ (n = 19–23; X = Na–Cl) clusters. The calculations are performed using the density functional theory with the PBE exchange–correlation energy functional. The results reveal that the most stable structures of $Ni_{n-1}X$ (X = Na, Mg, Al, Si) clusters are all similar to those of corresponding Ni_n clusters, while there are substantial structural deformations of $Ni_{n-1}X$ (X = P, S, Cl) clusters. From the optimized results, a systematic analysis is carried out to obtain the relative stability, charge transfer, magnetic moments, density of states, electron affinity and ionization potential of $Ni_{n-1}X$ clusters. Our findings also suggest how to change the stability, electronic and magnetic properties by doping different atoms in Ni clusters.

Keywords First-principles · Magnetic property · Charge transfer · Density of states · Stability

1 Introduction

Over the past decade, a lot of emphasis has been paid to the study of the physical and chemical properties of atomic clusters, which are the aggregates of atoms containing from a few to a few thousand atoms [1]. Studies on these clusters provide a unique perspective to understand the evolution of cluster electronic structure from that of atoms in the bulk and possibility to study the physicochemical properties as a function of cluster size. In recent years, transition metal (TM) clusters are widely used as structural materials, magnetic materials, and chemical catalysis. With the maturity of cluster theory, studies on single cluster have not been able to satisfy the discussion demand of cluster science. Therefore, researchers begin to further study the TM alloy clusters owing to their potential applications in catalysis, magnetic storage, optical and medical fields. At the nanoscale, the TM alloy clusters exhibit unusual electronic, magnetic and catalytic performances due to their particular chemical and physical properties, which can be controlled by changing the chemical composition and size. Consequently, the structures, electronic properties and magnetism of the TM alloy clusters have become one of the most active research subjects in the field of cluster physics. Among the TM alloy clusters, Ni-doped clusters have received great attention because the properties of doped clusters can be controlled by the selection of doped elements, the improvement of cluster stability, and the change of magnetic moments [2–4].

In general, the artificial introduction of impurity atoms into metal clusters is the basic method for studying the doping properties. And recent studies demonstrate that the chemical and electronic properties of TM clusters can be tuned by doping. It is very important to study TM-doped clusters at the atomic scale for exploring the reaction mechanism of catalysts and designing novel magnetic materials. Recently, some studies of Ni-doped clusters are focused on the physical, electronic and magnetic properties [5–10]. It is a known fact that the atomic radius decreases from left to right for the elements with the increase in the number

Wei Song and Peng-fei Ma contributed equally.

✉ Wei Song
chemsw@163.com

✉ Jin-long Wang
396292346@qq.com

1 School of Science, Henan Institute of Technology, Xinxiang 453003, People's Republic of China

2 School of 3D Printing, Xinxiang University, Xinxiang 453003, People's Republic of China

3 School of Physics and Electronic Engineering, Xinxiang University, Xinxiang 453003, People's Republic of China

4 Institute of Theoretical Chemistry, Jilin University, Changchun 130012, Jilin, People's Republic of China

of electrons in the outermost shell. In this study, the third periodic elements-doped nickel clusters are selected mainly because of their unique electronic properties. Sodium and magnesium are important alkali and alkaline earth metals. Owing to its active chemical properties, Na is commonly used in medical treatment and nuclear reactors, while Mg, with its lightweight and low strength, is commonly used in aerospace. Aluminum is the most abundant metallic element in the crust. Due to the special properties of Al and its alloys, it is widely used in aviation, architecture and automobile. And silicon is a crucial semiconductor material. In addition, phosphorus, sulfur and chlorine also play significant roles in agricultural production and industrial development. Therefore, many significant improvements have been achieved in the study of the structural, electronic and magnetic properties of the Ni-X (X = Na, Mg, Al, Si, P, S and Cl) systems. A few years ago, Deshpande et al. reported the magnetic properties of small $Ni_{13-n}Al_n$ clusters with n = 0–13 calculated in the framework of density functional theory. The cluster magnetic moment decreases with the sequential substitution of Ni by Al atoms, which can be attributed to a greater degree of hybridization that forces the pairing of the electrons in the molecular orbitals of Ni and Al [11]; In another study, Shah et al. investigated the equilibrium structure, electronic and magnetic properties of $Ni_{3n}Al_n$ (n = 1, 8) clusters using ab initio total-energy calculations based on density functional theory. They found the magnetic moment per atom in these clusters was significantly enhanced with respect to the bulk and a net transfer of charge from the d-type orbital of Ni to the p-type orbital of Al [12]. Experimentally, Zhang et al. studied the structural effects of sodium cations in polynuclear, multicubane-type mixed Na–Ni complexes [13]; later, after Mg and Ni nanoparticles were fabricated by hydrogen plasma metal reaction, Mg-rich Mg_xNi_{100-x} ($75 < x < 100$) materials were synthesized from these metal nanoparticles to study the synergistic effects for hydrogen storage in these samples to show both good kinetics and high capacity by Shao et al. [14]; recently, Kursun et al. reported the influence of the mechanical alloying on the microstructure, thermal and mechanical features of $Mg_{65}Ni_{20}Y_{15-x}Si_x$ (x = 1, 2, 3) alloys. The Mg-based alloys are produced by mechanical alloying techniques from mixtures of pure crystalline Mg, Ni, Y and Si powders. These alloys are investigated by using a variety of analytical techniques including X-ray diffraction (XRD), scanning electron microscopy (SEM), energy-dispersive spectrometry (EDX) and differential scanning calorimetry (DSC) [15] and so on [16].

Although more and more researchers systematically and deeply investigate the Ni alloy clusters, how to choose the doping elements, composition, atomic arrangement and size to obtain the new electromagnetic properties is still a key problem in cluster application research. And the theoretical study of Ni alloy clusters provides detailed electronic structure information for the properties of chemical adsorption and catalytic reaction. Especially for the study of medium-scale Ni alloy clusters, it can not only serve as a bridge between atom-scale and macro-solid but also provide a platform for the study of many catalytic reactions. However, as far as we know, the structures, electronic and magnetic properties of X-doped (X = Na, Mg, Al, Si, P, S and Cl) medium-scale Ni clusters have not been investigated until now. Therefore, in this article, the lowest-energy structures of pure Ni_n (n = 19–23) clusters are optimized first based on the previous calculation results. For X-doped (X = Na, Mg, Al, Si, P, S and Cl) Ni clusters, we examine the changes in the structural, electronic and magnetic properties using the density functional theory with the PBE exchange–correlation energy functional. The purpose of the present work is to address how X atoms (X = Na, Mg, Al, Si, P, S and Cl) doping affects the host clusters, how the resulting binding energy is compared with the pure clusters, and how electronic properties such as the ionization potential, electron affinity, charge transfer and magnetic moments are modified. The article is organized as follows. Section 2 briefly describes the theoretical methods used in this work. In Sect. 3, we present the lowest-energy structures and discuss the stability, electronic and magnetic properties of these clusters. Finally, the conclusions of this work are made in Sect. 4. We hope that our work will be useful for understanding the influence of material structure on its properties and can offer relevant information for further experimental and theoretical studies.

2 Computational theory

Density functional theory (DFT) is based on the electronic density of the system, which not only considers the electronic interaction but also avoids the time-consuming shortage of large system. It can be said that DFT has opened up a new way for the calculation of molecular properties. For the development of cluster science, theoretical calculation plays an extremely important role. Among them, DFT is a suitable computational method to treat clusters containing transition metals and plays an important role in quantum mechanics. Therefore, in this study, our calculations presented here are carried out using the DFT, as implemented in the VASP code [17–20]. In the VASP calculation, we employ the spin polarized generalized gradient approximation (GGA) exchange–correlation potential as parametrized by Perdew, Burke and Ernzerhof (PBE). Valence electrons are treated explicitly and their interactions with ionic cores are described by the Projector Augmented Wave (PAW) pseudopotential. The energy convergence criterion for the structure relaxation calculation is 10^{-5} eV. And the

internal coordinates are relaxed till the Hellmann–Feynman forces are less than 0.01 eV/Å. The clusters are placed in a cubic supercell with an edge of 20 Å, and periodic boundary conditions are imposed. Because of the large supercell and cluster calculation, interaction between the cluster and its replicas in neighboring cells can be negligible, and the Brillouin zone integration is carried out using only the Γ point. In our study of the cluster magnetic properties, we note that we only compute the atomic spin magnetic moments, i.e., spin–orbit interactions are not taken into account.

In order to predict the relative stability of the neutral and ionic $Ni_{n-1}X$ (n = 19–23; X = Na–Cl) clusters, we have calculated the binding energy per atom (BE) for the lowest-energy structures by using the following formulas:

$$BE(Ni_{n-1}X) = [(n-1)E(Ni) + E(X) - E_{total}(Ni_{n-1}X)]/n$$

$$BE(Ni_{n-1}X^{+/\cdot}) = [(n-1)E(Ni) + E(X^{+/\cdot}) - E_{total}(Ni_{n-1}X^{+/\cdot})]/n$$

where E(Ni), E(X), E($X^{+/\cdot}$), E_{total} ($Ni_{n-1}X$) and E_{total} ($Ni_{n-1}X^{+/\cdot}$), respectively, represent the total energies of the most stable Ni, X, $X^{+/\cdot}$, $Ni_{n-1}X$ and $Ni_{n-1}X^{+/\cdot}$ clusters. For illustrating the influence that the impurity atom X has on the relative stability of Ni_n clusters, the BE of the lowest-energy structures for Ni_n clusters are also calculated by the following formula:

$$BE(Ni_n) = [nE(Ni) - E_{total}(Ni_n)]/n$$

$$BE(Ni_n^{+/\cdot}) = [(n-1)E(Ni) + E(Ni^{+/\cdot}) - E_{total}(Ni_n^{+/\cdot})]/n$$

where E(Ni), E($Ni^{+/\cdot}$), E_{total} (Ni_n) and E_{total} ($Ni_n^{+/\cdot}$), respectively, represent the total energies of the most stable Ni, $Ni^{+/\cdot}$, Ni_n and $Ni_n^{+/\cdot}$ clusters. By this definition, the larger the value of the BE is, the more stable the cluster is.

3 Results and discussion

3.1 Ni_n (n = 19–23) cluster structures

The lowest-energy structures of the pure Ni_n clusters that have n = 19–23 are optimized on the basis of previous calculation results [21]. Our calculation shows that the lowest-energy structure of Ni_{19} is a perfect double-interpenetrating icosahedron, which has three parallel pentagonal rings stacked in a 1–5–1–5–1–5–1 sequence. The most stable structures of Ni_{20} and Ni_{21} are formed by adding one and two atoms to the cluster side face in the waist of Ni_{19}. And the lowest-energy structure of Ni_{22} is considered as adding one more atom above the center of the equilateral triangle of Ni_{21}, leading to a tetrahedron unit on the cluster side face. Similarly, Ni_{23} is viewed as adding one atom to Ni_{22}, showing as a Ni_4 segment to Ni_{19}. The calculation of all lowest-energy structures for Ni_n (n = 19–23) clusters is using a combination method of genetic algorithm (GA) searching with a tight-binding potential and the DFT calculations, as shown in Fig. 1.

3.2 $Ni_{n-1}X$ (n = 19–23; X = Na–Cl) cluster structures

It is well known that the research of the most stable structures of alloy clusters remains a challenge due to the huge amount of isomers. Especially, if one metal is magnetic, the study becomes more complicated because several spin states must be investigated. There is always a danger of missing the lowest energy isomer resulting from the limit of our current computational power. Nevertheless, the reliability of the lowest-energy structures obtained is strongly dependent on the selection of the initial cluster geometries. Since the number of possible geometries increases dramatically with cluster size. Firstly, we choose initial structures based on the lowest-energy structures in our previous studies in order to find as many as possible reasonable starting points, then we

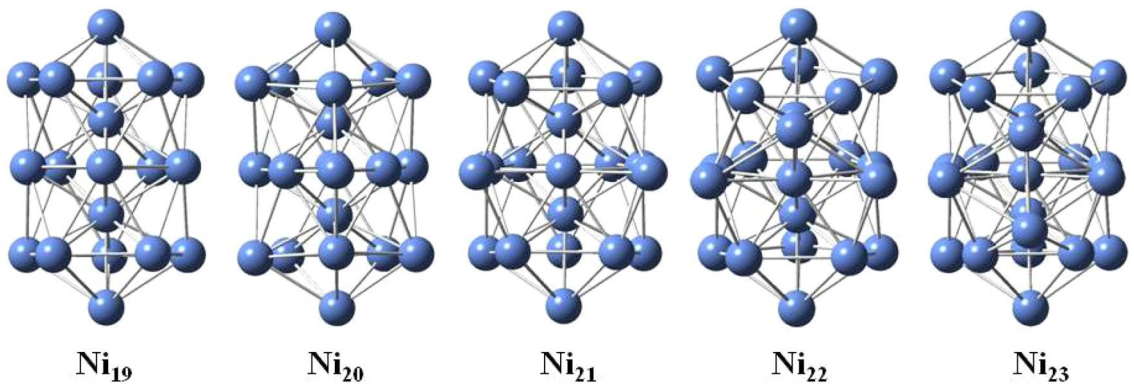

Fig. 1 Lowest-energy structures of the Ni_n (n = 19–23) clusters calculated at the DFT–PBE level

carried out an extensive search of the low-energy isomers of $Ni_{n-1}X$ clusters by considering all substituted doping positions for each cluster size. Finally, for each initial structure of the low-lying isomers, the structure is repeated without any symmetry restriction using DFT calculations and the lowest-energy structures of $Ni_{n-1}X$ ($n = 19$–23; X = Na–Cl) clusters are determined and presented in Figs. 2 and 3.

Now we discuss the results on X-doped Ni_n clusters. As presented in Fig. 2, we can observe the same doping position for X-doped (X = Na, Mg) Ni_n clusters. The lowest-energy structures of $Ni_{n-1}Na$ and Ni_{n-1} Mg are obtained by replacing a top atom of the initial structures. For $Ni_{n-1}Al$ clusters, the most stable structure of $Ni_{18}Al$ is still to replace a top atom. $Ni_{20}Al$ and $Ni_{21}Al$ can be viewed as substitution of a Ni atom by an Al to the top layer of Ni_{21-22}, while $Ni_{19}Al$ and $Ni_{22}Al$ are being formed, in which an Al is found to the position of the waist. However, it is found from observing Fig. 3 that all Si atoms prefer to be doped at the center rather than at the surface. According to above discussions on $Ni_{n-1}X$ clusters, we have found that the most stable structures of $Ni_{n-1}X$ (X = Na, Mg, Al, Si) clusters keep similar frameworks with the classical double-icosahedron of Ni_n clusters. Moreover, the X atom has tended to become a part of the clusters and can be looked upon as a substitutional impurity in the pure Ni_n clusters. Nevertheless, the original and most stable structures of Ni_n clusters begin to be broken after doping X (X = P, S, Cl) atoms. And there is substantial structural deformation for most of the lowest-energy structures of $Ni_{n-1}X$ clusters. Among them, Cl atom doping is most obvious. This change in structural deformation can be understood by the decreased radius of X (X = P, S, Cl) atoms and because of the stronger electron absorption capacity of them. Later, we will discuss this in detail in the charge transfer section.

The calculated bond lengths for the lowest-energy structures of $Ni_{n-1}X$ clusters are listed in Table 1. From Table 1, we can obverse that the effects of scale on bond lengths are not very obvious for all $Ni_{n-1}X$ clusters. From the analysis of details, we have found that the bond lengths increase slightly with the increase in clusters size for X-doped (X = Na, Mg, Al, Si) Ni_n clusters. And the bond lengths show the oscillation behavior and the difference is less than 0.1 Å for $Ni_{n-1}X$ (X = P, S, Cl) clusters. In particular, we also have observed the order of the bond lengths from the longest to the shortest is Na, Mg, Al, Si, P, S, Cl-doped Ni_n clusters. This is because the radius of atoms decreases gradually from left to right for elements of the same period. Furthermore, the bond lengths of Ni–S and Ni–Cl are similar, which is due to the serious deformation of the initial structures caused by Cl atom doping. In general, the shorter bond length can lead to higher bond tightness and more stability of the clusters.

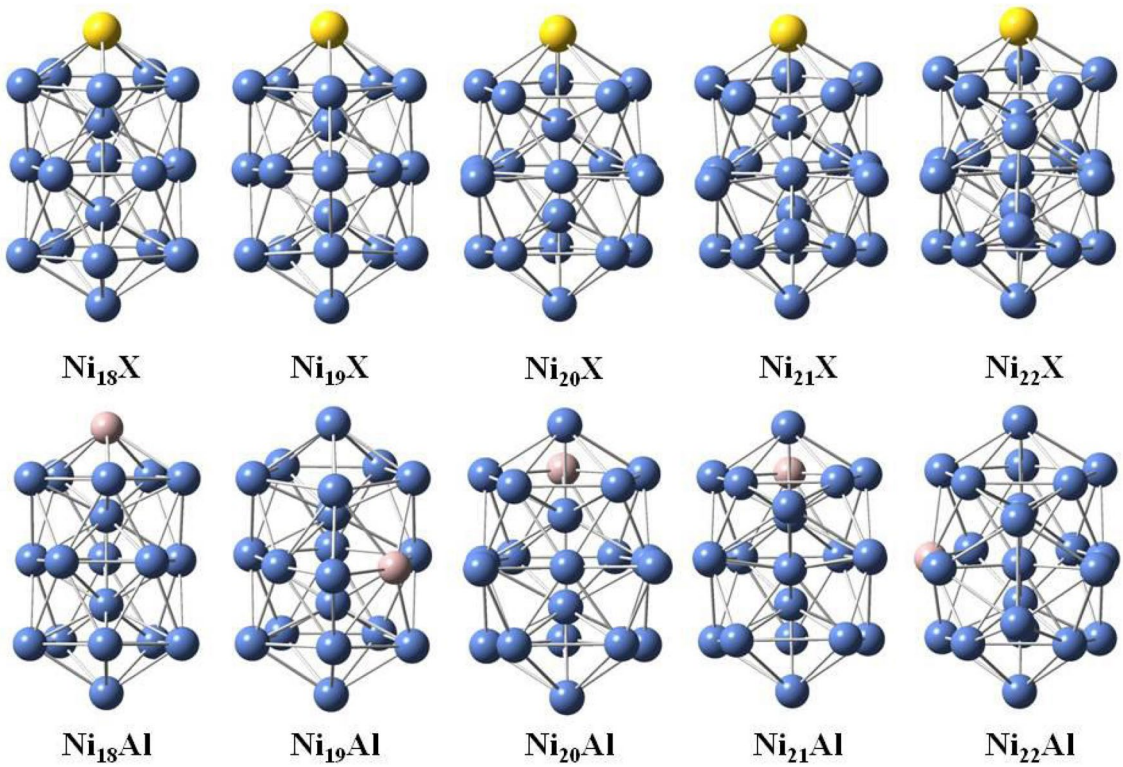

Fig. 2 Lowest-energy structures of $Ni_{n-1}X$ (X = Na, Mg) and $Ni_{n-1}Al$ ($n = 19$–23) clusters calculated at the DFT–PBE level

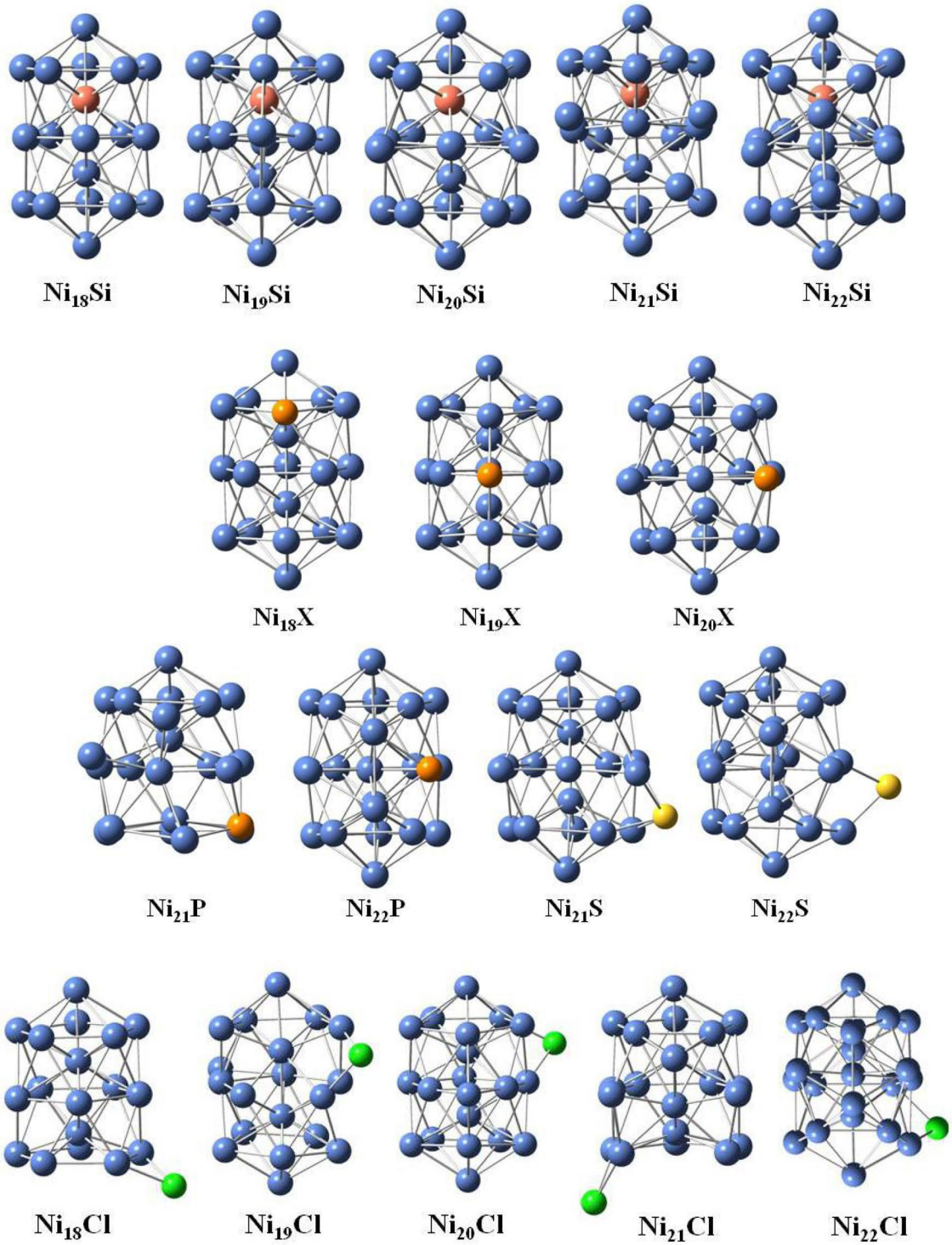

Fig. 3 Lowest-energy structures of $Ni_{n-1}Si$, $Ni_{n-1}X$ (*X* = P, S) and $Ni_{n-1}Cl$ (*n* = 19–23) clusters calculated at the DFT–PBE level

Thus the stability of doping S and Cl atoms is higher than that of doping other atoms, which is in close agreement with our results for the binding energy later on.

3.3 Relative stability

Considering the importance of cluster stability in the synthesis of cluster-based nanomaterials, we have focused on the energetics and stability of X-doped Ni_n clusters in this

Table 1 The Bond length (Å) of Ni-X for $Ni_{n-1}X$ ($n = 19–23$; $X = Na–Cl$) clusters

Bond length (Å)	$Ni_{18}X$	$Ni_{19}X$	$Ni_{20}X$	$Ni_{21}X$	$Ni_{22}X$
Na	2.99	3.05	3.09	3.12	3.18
Mg	2.65	2.69	2.70	2.77	2.80
Al	2.48	2.50	2.52	2.53	2.55
Si	2.22	2.25	2.27	2.29	2.30
P	2.33	2.18	2.21	2.25	2.32
S	2.21	2.25	2.17	2.21	2.10
Cl	2.21	2.20	2.22	2.22	2.23

section. The physical significance of binding energy is that the energy is obtained by placing an atom on an existing cluster, which can be utilized to characterize the relative stability of clusters. The calculated binding energy per atom (BE) values is provided in Fig. 4. It is found from observing Fig. 4 that the BE values of neutral Ni_n and $Ni_{n-1}X$ clusters increase monotonically as a function of cluster size. The higher BE reflects its higher stability, indicating that the stability of large clusters is stronger. This is due to the increasing average coordination number and effective hybridization, which makes the interaction between atoms in clusters stronger. For ionic clusters, the overall change trend of BE curves increases with the increase in cluster size, especially for Na, Mg, Al and Si atom doping, the oscillation of the curve is not obvious, while for $Ni_{n-1}X^{+/-}$ ($X = P, S, Cl$) clusters, the BE values show an oscillating behavior on certain scales. Next, we have analyzed and discussed the causes of the phenomenon. Because there are many factors that affect the binding energy of clusters, such as geometry, charge transfer, impurity effect and so on. From the results of our calculation at present, it can be seen that in the presence of a certain charge, if the geometry and impurity effect exist at the same time, the impurity effect plays a major role in the binding energy. This is the reason that we can change the stability, structure and properties of clusters by doping different impurities. In addition, for pure Ni_n clusters, we have observed that the BE of neutral clusters is lower than that of ionic clusters. This may have something to do with the electron configuration of the nuclei in the cluster. For the same size, the order of the BE curves is $BE^+ > BE > BE^-$, showing that the stability of decreasing one anti-bonding electron is stronger than that of increasing one bonding electron for neutral clusters. However, for $Ni_{n-1}X$ clusters, the order of the BE curves can be divided into three regions: $BE^+ > BE^- > BE$ for doping Mg and Si atoms; $BE^- > BE > BE^+$ for doping Na and Al atoms; $BE^+ > BE > BE^-$ for doping P, S and Cl atoms. This further indicates that the types of doped atoms affect the electron configuration of the host clusters to some extent. Finally, for all neutral and ionic Ni_n clusters, we also have found that the BE curves increase with the substitution of one Ni atom by one Si or P atom. Therefore, it is clear that the Si and P-doped indeed contribute to strengthen the energetic stability of Ni_n clusters. However, the BE curves show an opposite trend for doping Na and Mg atoms, which indicates that the Na and Mg-doped can weaken the stability of the Ni_n clusters. Unfortunately, as an overall, the calculated BE values do not show some regularity for doping Al, S and Cl atoms. Thus, to some extent, the types of doped atoms can determine the stability of the host clusters. And the concrete influence degree and the reason still remain to be studied.

3.4 Charge transfer

Besides being an intuitive scheme for visualizing atoms in molecules, Bader's definition is often useful for charge analysis. The charge distribution can be used to determine multipole moments of interacting atoms or molecules. Bader charge analysis has also been used to define the hardness of atoms, which can be used to quantify the cost of removing the charge from an atom. To explore in better detail the electronic properties, we carry out Bader charge analysis for the local charge of the most stable structures of $Ni_{n-1}X$ clusters, which can provide a reliable charge transfer information. Here, the charge transfer of the X atoms and Ni clusters is displayed in Fig. 5. The reason for the charge transfer is that the atoms in the unequal space are affected by different potential fields, which causes some of the atoms to lose electrons and some of the others to gain electrons. It is well known that the directionality of charge transfer is related to the electronegativity of an element. The electronegativity takes ionization potential and electron affinity into account, which is used to indicate the relative strength of the ability to attract electrons when a chemical bond is formed between two different atoms. Generally speaking, the greater the electronegativity is, the stronger the ability to attract electrons is. For elements of the same period, the electronegativity increases from left to right. Thus the electronegativity of Ni (1.91) is larger than metal atoms for Na (0.93), Mg (1.31) and Al (1.61), almost equal to Si atom (1.90), and smaller than the nonmetallic atoms for P (2.19), S (2.58) and Cl (3.16), respectively. As can be seen from Fig. 5, the charge transfer takes place from metal atoms (Na, Mg, Al) to Ni clusters, which may derive from the larger electronegativity of Ni with respect to metal atoms (Na, Mg, Al). On the contrary, the charge is transferred from the nonmetallic atoms (P, S, Cl) atoms to Ni clusters except Si atom; in other words, P, S and Cl in the most stable structures of $Ni_{n-1}X$ clusters obtain electronic charges from surrounding Ni atoms. Then we have analyzed the reasons for Si-doped Ni_n clusters including the following two aspects. On the one hand, the electronegativity of Ni atom is almost equal to that

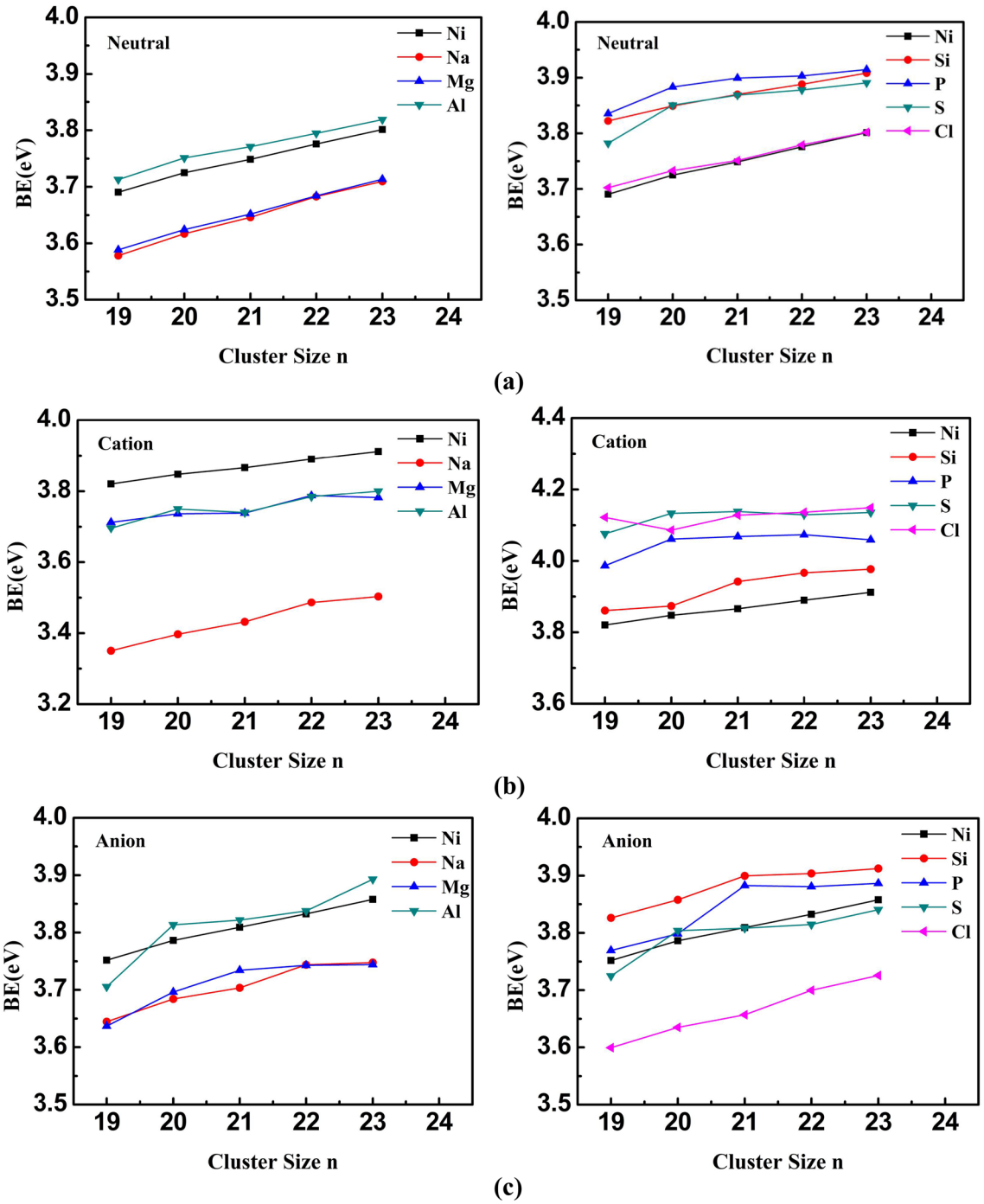

Fig. 4 Binding energy per atom (BE) of Ni_n and $Ni_{n-1}X$ ($n = 19$–23; X = Na–Cl) clusters for **a** neutral, **b** cation, and **c** anion

of Si atom; on the other hand, only Si atom prefers to dope in the center position of Ni clusters, and the encapsulated Si atom tends to interact with more Ni atoms with in-equivalent bond lengths and to saturate the dangling bonds of Ni atoms. So more electrons transfer from Si atom to Ni clusters.

In addition, we have observed that the amount of transfer charge is related to the number of extranuclear electrons of an atom, that is, the more the number of extranuclear electrons is, the greater the charge transfer is. So the most electrons can be lost by Al and Si atoms, corresponding to the local maxima of $Ni_{21}Si$ at a value of about 3.6e. However, as shown in Fig. 5, we also have found that more charge is transferred from Ni clusters to S atom compared to P and Cl atoms. Although the number of extranuclear electrons

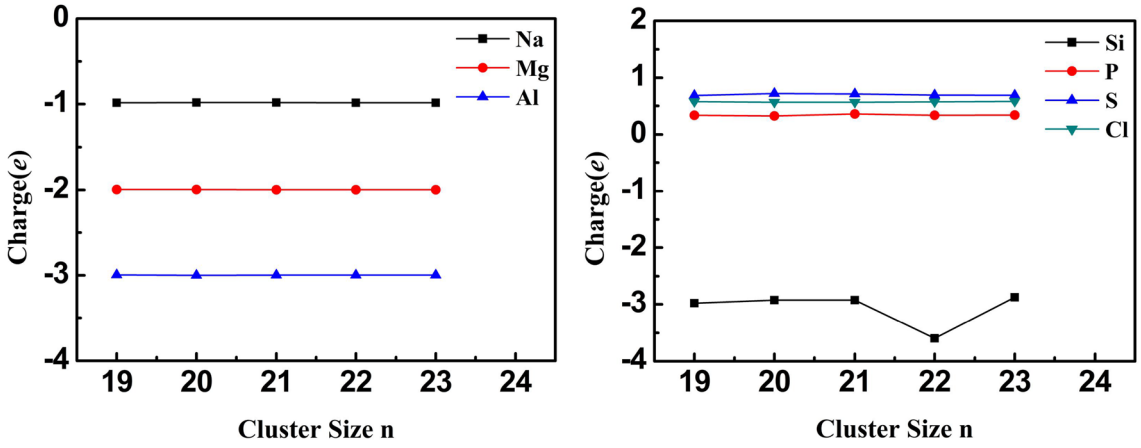

Fig. 5 Charge transfer (in units of *e*) between Ni_{n-1} clusters and X atoms ($n = 19–23$; $X =$ Na–Cl)

of Cl atom is more than that of S atom, the lowest-energy structures of $Ni_{n-1}Cl$ clusters are no longer based on double-icosahedron, resulting in obvious deformation and a fewer coordination number, so the charge transfer is less than S-doped.

3.5 Magnetic property

The study of magnetism in clusters is a two-step process, namely the identification of the lowest-energy structures and the determination of the respective electronic properties. The determination of the most stable structures of transition metal clusters is thus a vital step toward understanding cluster properties, such as catalytic and magnetic properties. Therefore, we study the magnetic properties of clusters based on the most stable structures and electronic properties.

The total magnetic moments calculated for the lowest-energy structures of Ni_n and $Ni_{n-1}X$ ($n = 19–23$; $X =$ Na–Cl) clusters are displayed in Fig. 6. Three distinct features of the total magnetic moments are founded. Firstly, as shown in Fig. 6, the neutral and ionic Ni_n clusters show a monotonous increase as a function of the cluster size, in the total magnetic moments. In addition, for the majority of X-doped Ni_n clusters, the total magnetic moments are lower than those of Ni_n clusters by 1 ~ 4 μ_B. However, $Ni_{18}Cl^{(0,\pm1)}$, $Ni_{22}Cl^{(0,\pm1)}$, $Ni_{20}Cl^{+}$ and $Ni_{21}Cl^{\cdot}$ clusters, the total magnetic moments become larger than those of $Ni_{19}^{(0,\pm1)}$, $Ni_{23}^{(0,\pm1)}$, Ni_{21}^{+} and $Ni_{22}^{\cdot}$ clusters, respectively. Finally, for the metal atoms (Na, Mg, Al) doping, the more the number of outermost electrons is, the more obvious the reduction of total magnetic moments is, and the trend is exactly the opposite for the nonmetallic atoms (Si, P, S, Cl) doping.

Therefore, these results indicate that the majority of substitution of X-atoms for Ni-atoms can weaken the magnetism of the host clusters and the degree of total magnetic moment reduction is also affected by the size of clusters and the type of doped atoms. Next, we analyze the reasons for this phenomenon. It is well known that the magnetic moments are generated by the motion of charged particles inside the matter, including electron orbital motions, electron spin motions, and nuclear spin motions. However, the orbital magnetic moment of an electron is far less than its spin magnetic moment, which is called the "orbital quenching effect". Thereby, the magnetic moment of the cluster is dominated by the spin magnetic moment [8, 22]. Generally speaking, atoms in a stable state (ground state), the extranuclear electrons can be arranged according to the principle of minimum energy as far as possible. In addition, not all the electrons can be crowded together; they must follow the Pauli exclusion principle and the Hund's rules. And the pseudopotentials for Ni, Na, Mg, Al, Si, P, S and Cl are generated using the valence configurations $3d^84s^2$, $3s^1$, $3s^2$, $3s^23p^1$, $3s^23p^2$, $3s^23p^3$, $3s^23p^4$ and $3s^23p^5$, respectively. The magnetism of Ni clusters is due to the d orbitals which are not filled with electrons. So the main reason for the total magnetic moment reduction is probably that the strong spd orbital hybridization for both Ni and *X* atoms, stronger interaction takes place, which results in partial quenching of the magnetic moments of Ni clusters. Certainly, the magnetic moments are related not only to the orbital hybridization but also to geometric structure, coordination number, bond length and charge transfer and so on. Next, we have analyzed and discussed the relationship between geometric structure, charge transfer and magnetic moment of clusters. In general, the greater the electron transfer between atoms, the more obvious the orbital hybridization phenomenon is, so the charge transfer and orbital hybridization affect the magnetic moment of the whole system. In our calculation, for the electron loss system (Na, Mg, Al, Si-doped Ni_n clusters), the more electrons the doped atom loses, the more obvious the hybridization is, and the more obvious the reduction of magnetic moment is. Therefore, the magnetic moments

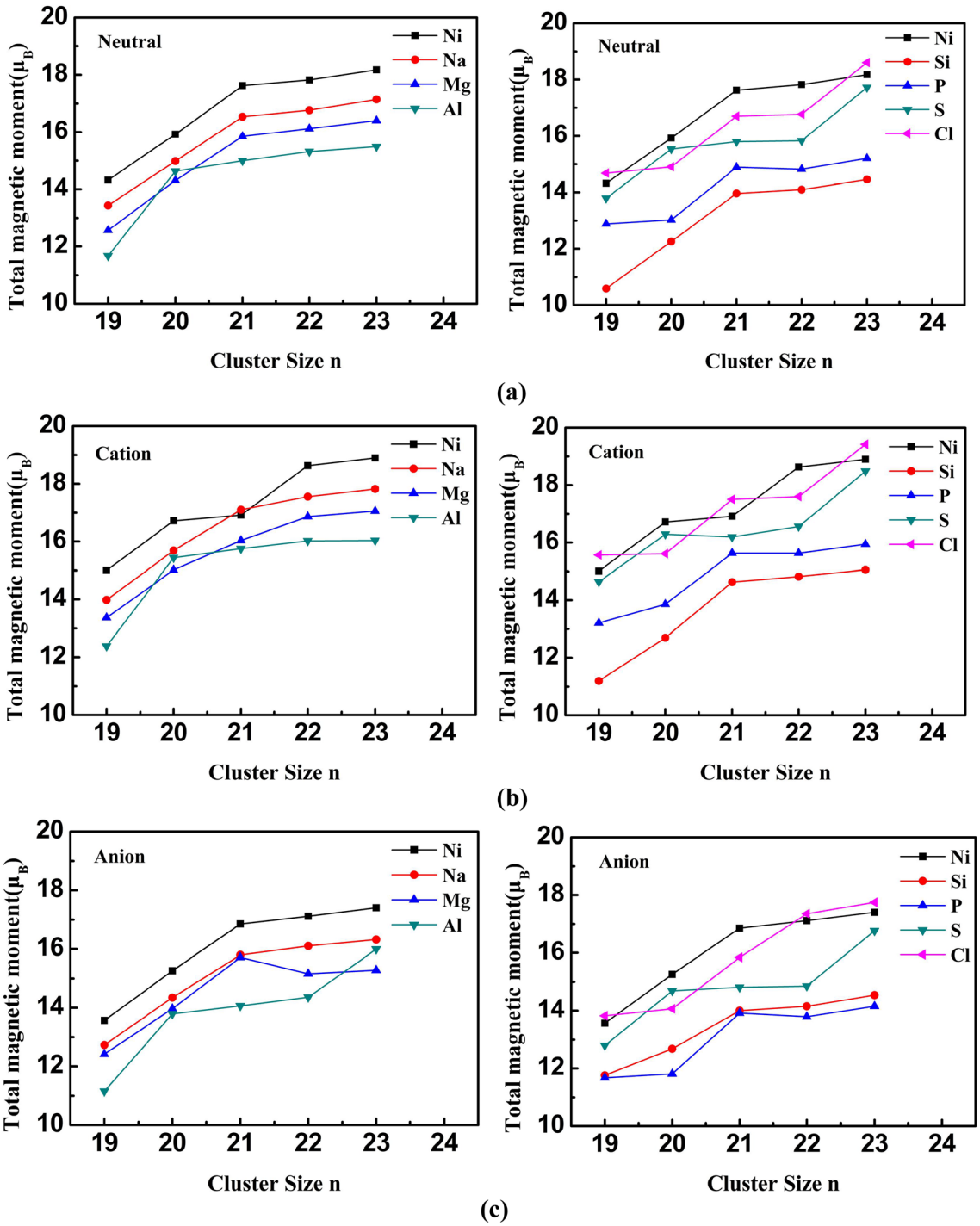

Fig. 6 The total magnetic moments (in units of μ_B) of Ni_n and $Ni_{n-1}X$ ($n = 19$–23; X = Na–Cl) clusters for **a** neutral, **b** cation, and **c** anion

of $Ni_{n-1}Al$ and $Ni_{n-1}Si$ clusters are the least because of losing the most electrons. On the contrary, for the system for getting electrons (P, S, Cl-doped Ni_n clusters), the more electrons doped atom gets, the more obvious the hybridization is, but the change of magnetic moment is weakened. Therefore, the magnetic moment of the $Ni_{n-1}P$ is the least because of getting the least electrons. At the same time, we also have found an interesting phenomenon that more charge is transferred from Ni clusters to S atom rather than Cl atom, but the magnetic moment is the largest for $Ni_{n-1}Cl$ clusters. This is mainly because the lowest-energy structures of the $Ni_{n-1}Cl$ clusters are seriously deformed and the coordination numbers are reduced, the total magnetic moments of some structures increase after Cl-doped Ni_n clusters. We will

analyze more details for the specific reasons in the density of state discussion.

3.6 Density of states (DOS)

The density of state (DOS) represents the number of electrons allowed in the unit energy range, that is, the distribution of electrons in a certain energy range. DOS can reflect the distribution of electrons in each orbit, the interaction between atoms, and the information of chemical bonds. Therefore, in this study, we can understand the electronic origin of the cooperative effect Ni-X hybridization by analyzing DOS and identify changes in the electronic and magnetic properties of the clusters. To further understand the reasons for the change of the total magnetic moments, we can plot the projected density of states (PDOS) for the neutral and ionic Ni_{23}, $Ni_{22}Na$ and $Ni_{22}Cl$ clusters as representatives in Fig. 7a–c. From the PDOS analysis, it can be concluded that 3d orbitals interactions have a strong influence on the total magnetic moments of these clusters, but the interactions among the 3s and 3p orbitals with 3d orbitals have little effect on their magnetic moments. In general, the relative shifts between the spin up and down of electrons can be the degree of the spin splitting of the density of states, the stronger the polarization and the greater the magnetism. It can be seen from Fig. 7a, Ni 3d orbitals show a peak near the Fermi level for Ni_{23} cluster. However, the Ni 3d orbital peaks broaden for Ni_{23}^{+} cluster and shorten for Ni_{23}^{-} cluster, respectively. As a result, the total magnetic moments of Ni_{23}^{+} cluster increase and that of Ni_{23}^{-} cluster decrease. These are consistent with the calculated total magnetic moments with 18.173 μ_B, 18.892 μ_B and 17.402 μ_B for Ni_{23}, Ni_{23}^{+} and Ni_{23}^{-} clusters, respectively. Similarly, we also have found from observing Fig. 7b-c that the 3d orbital peaks shorten for Na-doped and broaden for Cl-doped Ni_{23} clusters, which explains the lower and higher magnetic moments

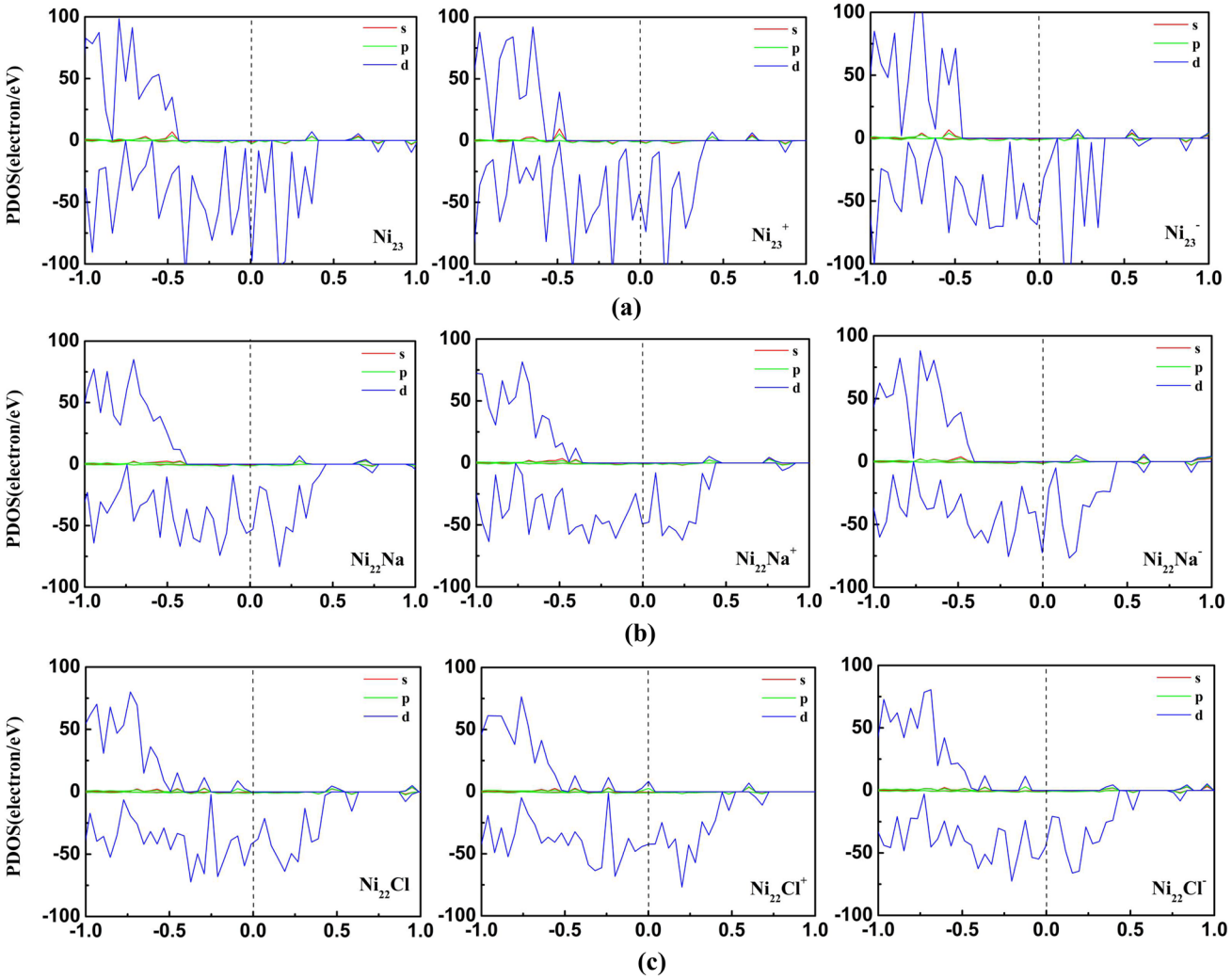

Fig. 7 The projected density of states (PDOS) of the neutral, cationic and anionic for **a** Ni_{23}, **b** $Ni_{22}Na$, and **c** $Ni_{22}Cl$ clusters

of $Ni_{22}Na$ and $Ni_{22}Cl$ clusters than those of Ni_{23} cluster, respectively.

To explore in better detail the magnetism, we have also carried out the local density of states (LDOS) for the neutral and ionic $Ni_{22}Na$ and $Ni_{22}Cl$ clusters (Fig. 8a-b). It can be seen from Fig. 8, the degree of the spin splitting of $Ni_{22}Na/Ni_{22}$ and $Ni_{22}Cl/Ni_{22}$ is similar to that of $Ni_{22}Na$ and $Ni_{22}Cl$, respectively. It implies a weak hybridization between s–d and p–d orbitals at the Fermi level, which also shows that the magnetism of $Ni_{22}Na$ and $Ni_{22}Cl$ clusters is derived from Ni atoms.

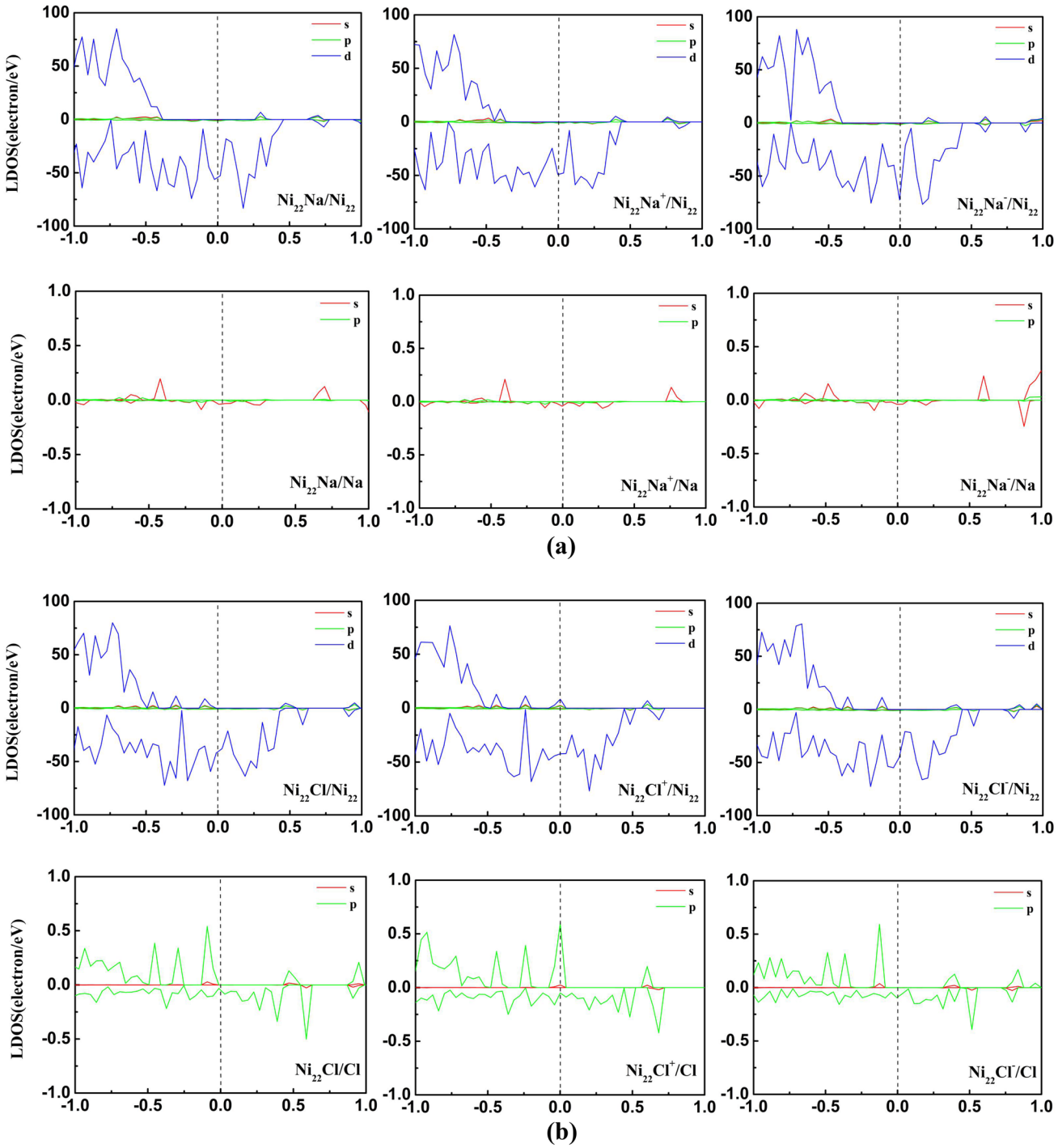

Fig. 8 The local density of states (LDOS) of the neutral, cationic and anionic for **a** $Ni_{22}Na$, and **b** $Ni_{22}Cl$ clusters

3.7 Electron affinity and ionization potential

It is well known that the electron affinity (EA) of elements reflects the degree of difficulty for obtaining electrons from atoms of elements. The smaller the EA of an atom is, the greater the tendency of the atom to gain electrons is. While the ionization potential (IP) can be used to measure the chemical reactivity and metallicity of the elements. The larger the IP is, the harder it is for an element to lose electrons. In other words, the smaller EA and the larger IP can indicate the nature of weaker metallicity and the stronger nonmetallicity of the element. Therefore, the EA and IP play an important role as a quantitative measure of the metallic and nonmetallic properties of the elements.

The EA and IP are calculated using the ground-state energies of the neutral and cationic/anionic clusters and thus correspond to the adiabatic electron affinity (AEA) and the adiabatic ionization potential (AIP), respectively. These equations are defined as follows:

$$\mathrm{AEA} = E(\text{optimized neutral}) - E(\text{optimized anion}).$$

$$\mathrm{AIP} = E(\text{optimized cation}) - E(\text{optimized neutral}).$$

Where E is the total energy of the corresponding system. The AEA and AIP values have been calculated based on the lowest-energy structures of the neutral and ionic of Ni_n and $Ni_{n-1}X$ ($n = 19$–23; X = Na–Cl) clusters and displayed in Fig. 9a, b, respectively.

The AEA values for pure Ni_n clusters are all around 3.2 eV plotted in Fig. 9a, indicating that the effect of scale is not obvious. When X-doped Ni_n clusters, the AEA values are reduced as a whole, which indicates that the stability of $Ni_{n-1}X$ clusters is enhanced. And $Ni_{19}P$ corresponds to the local minima value about 1.23 eV, exhibiting that it is the stronger nonmetallicity.

In addition, as can be seen from Fig. 9b, we have observed the AIP values increase for $Ni_{n-1}X$ excluding $Ni_{n-1}Na$ clusters. The AIP values of $Ni_{19}Si$ and $Ni_{19}S$ are calculated to be more than 6.0 eV, which are the maxima value, indicating

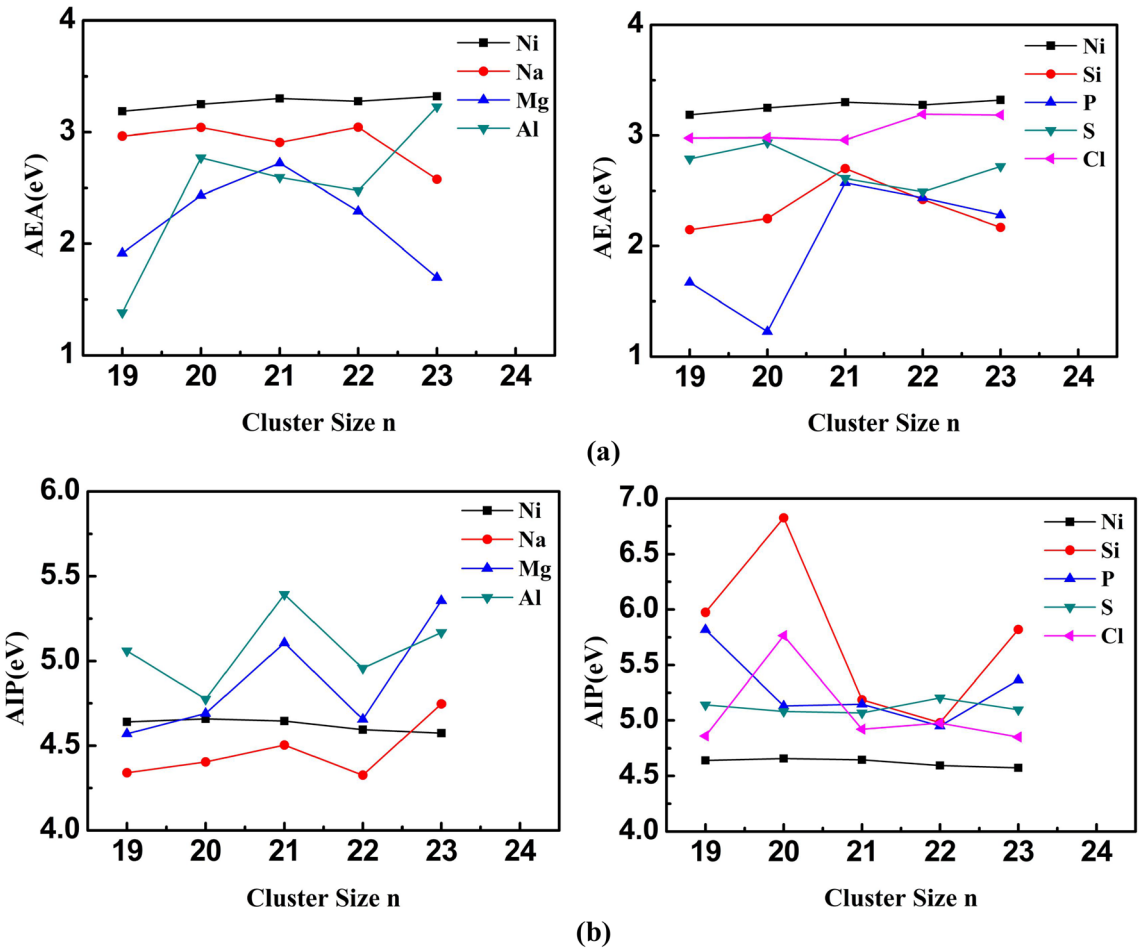

Fig. 9 **a** The adiabatic electron affinity (AEA) and **b** the adiabatic ionization potential (AIP) of Ni_n and $Ni_{n-1}X$ ($n = 19$–23; X = Na–Cl) clusters

that these clusters are difficult to lose electrons and the weaker metallicity.

Finally, the curves of the AEA and AIP show an oscillating behavior with the increase in cluster size and the difference of doped atoms. And there is no certain regularity to be found, so we need to carry out further analysis and discussion in future work.

4 Summary

Our systematic investigation on the neutral and ionic $Ni_{n-1}X$ (n = 19–23; X = Na–Cl) clusters employs the density functional theory with the PBE exchange–correlation energy functional. All calculated results can be summarized as follows:

(1) The most stable structures of $Ni_{n-1}X$ (X = Na, Mg, Al, Si) clusters are all similar to those of corresponding Ni_n clusters, while there are substantial structural deformations of $Ni_{n-1}X$ (X = P, S, Cl) clusters.

(2) The binding energy per atom (BE) curves increase and oscillate for neutral and ionic clusters as a function of cluster size, respectively. We have found that the BE curves increase with the substitution of one Ni atom by one Si or P atom. However, the BE curves show an opposite trend for doping Na and Mg atoms. Overall, the BE values do not show some regularity for doping Al, S and Cl atoms.

(3) The charge transfer takes place from metal atoms (Na, Mg, Al) to Ni clusters. On the contrary, the charge is transferred from the nonmetallic atoms (P, S, Cl) atoms to Ni clusters except Si atom. Most electrons can be lost by Al and Si atoms, corresponding to the local maxima of $Ni_{21}Si$ at a value of about 3.6e.

(4) For the majority of X-doped Ni_n clusters, the total magnetic moments are lower than those of Ni_n clusters by 1 ~ 4 μ_B. And the more the number of outermost electrons is, the more obvious the reduction of total magnetic moments is for the metal atoms (Na, Mg, Al) doping, and the trend is exactly the opposite for the nonmetallic atoms (Si, P, S, Cl) doping.

(5) The curves of the adiabatic electron affinity (AEA) and the adiabatic ionization potential (AIP) show an oscillating behavior with the increase in cluster size and the difference of doped atoms.

Acknowledgments The authors thank the National Natural Science Foundation of China for financial support (Grant Nos: 11705157 and 21673220). This work is also supported by the Natural Science Foundation of He'nan Department of Education (Grant No: 18B430012) and the ninth group of key disciplines in He'nan province (Grant No. 2018119). We are grateful to the Computing Center of Jilin Province for essential support.

References

1. R. Ferrando, J. Jellinek, R.L. Johnston, Nanoalloys: From theory to applications of alloy clusters and nanoparticles. Chem. Rev. **108**, 845–910 (2008)
2. H. Nady, H.M. Negem, Microstructure and corrosion behavior of electrodeposited NiCo, NiZn and NiCu nanocrystalline coatings in alkaline solution. Z. Phys. Chem **231**, 1159–1178 (2017)
3. L.S. Wu, H.B. Dai, X.P. Wen, P. Wang, Ni–Zn alloy nanosheets arrayed on nickel foamas a promising catalyst for electrooxidation of hydrazine. Chemelectrochem **4**, 1944–1949 (2017)
4. J. Teeriniemi, P. Taskinen, K. Laasonen, First-principles investigation of the Cu–Ni, Cu–Pd, and Ni–Pd binary alloy systems. Intermetallics **57**, 41–50 (2015)
5. J.M. Ortiz-Roldan, A.R. Ruiz-Salvador, S. Calero, F. Montero-Chacon, J. Segurado, I. Martin-Bragado, S. Hamad, Thermo-structural behaviour of Ni–Cr materials: Modelling of bulk and nanoparticle systems. Phys. Chem. Chem. Phys. **17**, 15912–15920 (2015)
6. X. Li, X.X. Wang, M.C. Liu, H.Y. Chen, Y.D. Yin, M.S. Jin, Construction of Pd–M (M = Ni, Ag, Cu) alloy surfaces for catalytic applications. Nano Res **11**, 780–790 (2018)
7. S. Datta, A.K. Raychaudhuri, T. Saha-Dasgupta, First principles study of bimetallic $Ni_{13-n}Ag_n$ nano-clusters (n=0–13): Structural, mixing, electronic, and magnetic properties. J. Chem. Phys. **146**, 1–8 (2017)
8. B. Zhu, D. Die, R.C. Li, H. Lan, B.X. Zheng, Z.Q. Li, Insights into the structural, electronic and magnetic properties of Ni-doped gold clusters: Comparison with pure gold clusters. J. Alloy. Compd. **696**, 402–412 (2017)
9. A. Mukhtar, M. Tun, H. Hu, L.P. Liu, T. Mehmood, B.S. Khan, Formation of metastable Co–Ni Alloy nanowires in electrodeposition. J Nanosci Nanotechno **18**, 1296–1302 (2018)
10. R.K. Singh, T. Iwasa, T. Taketsugu, insights into geometries, stabilities, electronic structures, reactivity descriptors, and magnetic properties of bimetallic Ni_mCu_{n-m} (m=1, 2; n=3–13) clusters: comparison with pure copper clusters. J. Comput. Chem. **39**, 1878–1889 (2018)
11. M.D. Deshpande, R. Pandey, M.A. Blanco, A. Khalkar, Magnetic properties of $Ni_{13-n}Al_n$ clusters with n=0–13. J. Nanopart. Res. **12**, 1129–1136 (2010)
12. V. Shah, D.G. Kanhere, Electronic structure and magnetic properties of $Ni_{3n}Al_n$ clusters. Phys. Rev. B **80**, 125419 (2009)
13. J. Zhang, P. Teo, R. Pattacini, A. Kermagoret, R. Welter, Structural effects of sodium cations in polynuclear, multicubane-type mixed Na–Ni complexes. Angew. Chem. Int. Edit. **49**, 4443–4446 (2010)
14. H.Y. Shao, C.G. Chen, T. Liu, X.G. Li, Phase, microstructure and hydrogen storage properties of Mg–Ni materials have synthesized from metal nanoparticles. Nanotechnology **25**, 135704 (2014)
15. C. Kursun, M. Gogebakan, H. Eskalen, Mechanical properties, microstructural and thermal evolution of $Mg_{65}Ni_{20}Y_{15-x}Six$ (x=1, 2, 3) alloys by mechanical alloys. Mater. Res. Express **5**, 036512 (2018)
16. J.N. Balaraju, V.E. Selvi, K.S. Rajam, Electrochemical behavior of nanocrystalline Ni-P alloys containing tin and tungsten. Prot. Met. Phys. Chem. **46**, 686–691 (2010)
17. G. Kresse, J. Hafner, Ab initio molecular dynamics for liquid metals. Phys. Rev. B **47**, 558–561 (1993)

18. G. Kresse, J. Furthmuller, Efficient iterative schemes for ab initio total-energy calculations using a plane-wave basis set. Phys. Rev. B **54**, 11169–11186 (1996)
19. P.E. Blochl, Projector augmented-wave method. Phys. Rev. B **50**, 17953–17979 (1994)
20. J.P. Perdew, K. Burke, M. Ernzerhof, Generalized gradient approximation made simple. Phys. Rev. Lett. **77**, 3865–3868 (1996)
21. W. Song, W.C. Lu, Q.J. Zang, C.Z. Wang, K.M. Ho, Double icosahedron-based motif of Ni_n (n=20–30). Int. J. of Quant. Chem. **112**, 1717–1724 (2012)
22. R. Trivedi, K. Dhaka, D. Bandyopadhyay, Study of electronic properties, stabilities and magnetic quenching of molybdenum-doped germanium clusters: A density functional investigation. RSC Adv. **4**, 64825–64834 (2014)